Determination of $^{12}C/^{13}C$ Ratios in Orion IRc2 Acetylene Isotopologues Using TOPSEGI and Quantum Chemical Calculations

Minkyu Lee
(Soongsil University)

In collaboration with
Jubin Park (OMEG / Soongsil University)
Sehoon Oh (OMEG / Soongsil University)
Myung-Ki Cheoun (OMEG / Soongsil University)
Se Young Park(OMEG / Soongsil University)

Motivation

➢ Acetylene is among the simplest organic molecules found abundantly in outer space.

Object		Measurement technique	Investigation Year	Range cm^{-1}	Range μm	Ref.
Planets	Jupiter	Cassini/CIRS mid infrared spectra	2006	670 ∼ 760	14.9 ∼ 13.2	(1)
	Saturn	ISO-SWS	1997	666.7 ∼ 714.3	15 ∼ 14	(2)
	Uranus	ISO (Infrared Space Observatory)	1998	694.4 ∼ 769.2	13 ∼ 14.4	(3)
	Neptune	Voyager 2/IRIS	1991	720 ∼ 740	13.9 ∼ 13.5	(4)
Satellites	Titan	TEXES	2017	742.9 ∼ 746.7	13.5 ∼ 13.4	(5)
Comets	Hyakutake	Infrared Telescope Facility at Mauna Kea Cryogenic echelle spectrometer (CSHELL)	1996	3282 ∼ 3288	3.047 ∼ 3.041	(6)
Carbon star	IRC +10216	TEXES	2008	714.29 ∼ 909.09	14 ∼ 11	(7)
Orion IRc2		SOFIA/EXES	2018	750.19 ∼ 771.60	13.33 ∼ 12.96	(8)

References— (1) Nixon et al. 2007; (2) de Graauw et al. 1997; (3) Encrenaz et al. 1998; (4) Bézard et al. 1991; (5) Bézard et al. 2022; (6) Brooke et al. 1996; (7) Fonfría et al. 2008; (8) Rangwala et al. 2018;

NOTE—We focus on the frequency ranges exhibiting infrared activity among various acetylene observation data.

Jupiter (Planet)

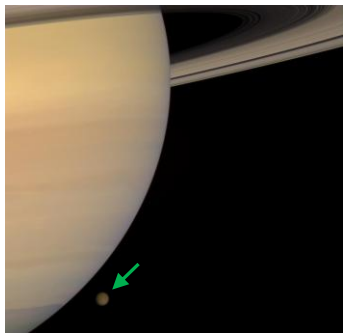

Saturn & Titan (Planet & Satellite)

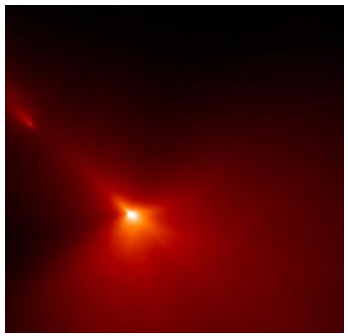

Hyakutake (Comet)

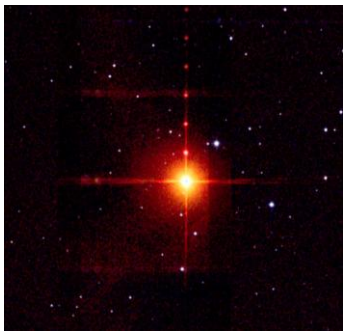

IRC +10216 (Carbon star)

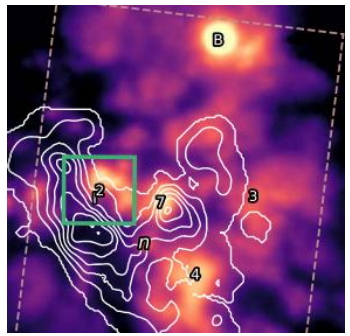

Orion IRc2

- Pentsak, E. O., Murga, M. S., & Ananikov, V. P. 2024, ACS Earth and SpaceChemistry, 8, 798
- Nickerson, Sarah, et al. "The mid-infrared molecular inventory toward orion IRc2." The Astrophysical Journal 945.1 (2023): 26.
- https://images.nasa.gov/

Motivation

- **Carbon, the primary element in acetylene** is mainly formed in thermonuclear fusion reaction at the stars of intermediate masses (from $\sim 0.8M_{\odot}$ to $8M_{\odot}$).
- 12C/13C is an important diagnostic tool for probing the Galactic chemical evolution or simply the **nucleosynthesis history** of the Galaxy. (AGB Star => (12C(p,γ)13N(β+)13C))
- Observations have shown that the carbon star Y CVn has a 12C/13C ratio of **3.5 (13C ≈ 22%)**

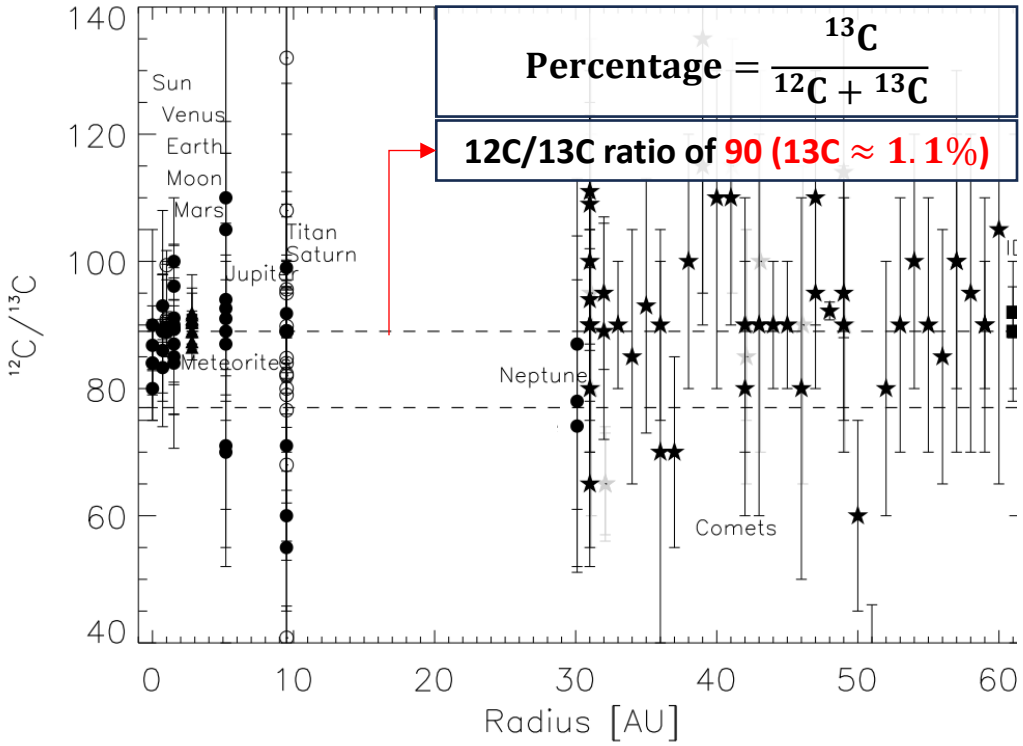

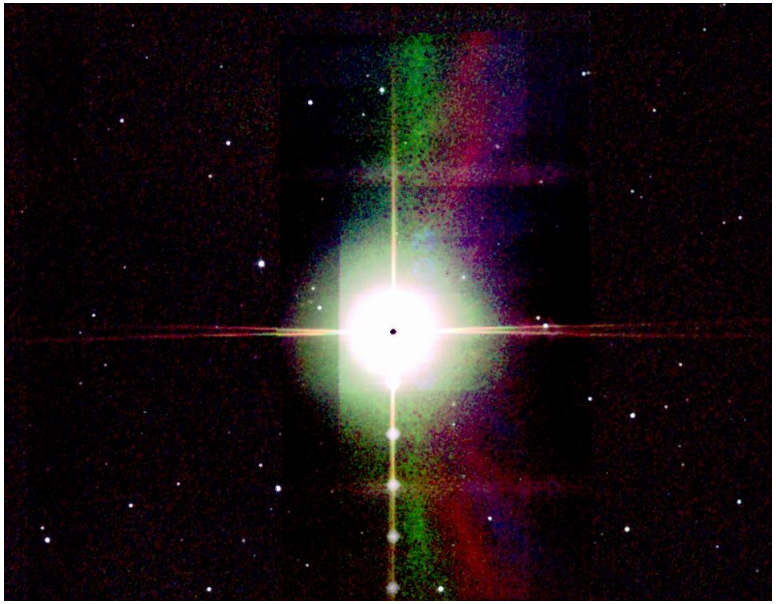

Y Cyn [La Superba]
(Carbon star)

- Pentsak, E. O., Murga, M. S., & Ananikov, V. P. 2024, ACS Earth and SpaceChemistry, 8, 798
- Woods, Paul M. "Carbon isotope measurements in the Solar System." arXiv preprint arXiv:0901.4513 (2009).
- Schöier, F. L., & Olofsson, H. (2000). The 12C/13C-ratio in cool carbon stars. arXiv preprint astro-ph/0005360.

Motivation

- IRc2 : The brightest source among the **'IRc' sources** in the KL nebula, a region of the **Orion Molecular Cloud. (Interesting point : Its nature remains unclear)**

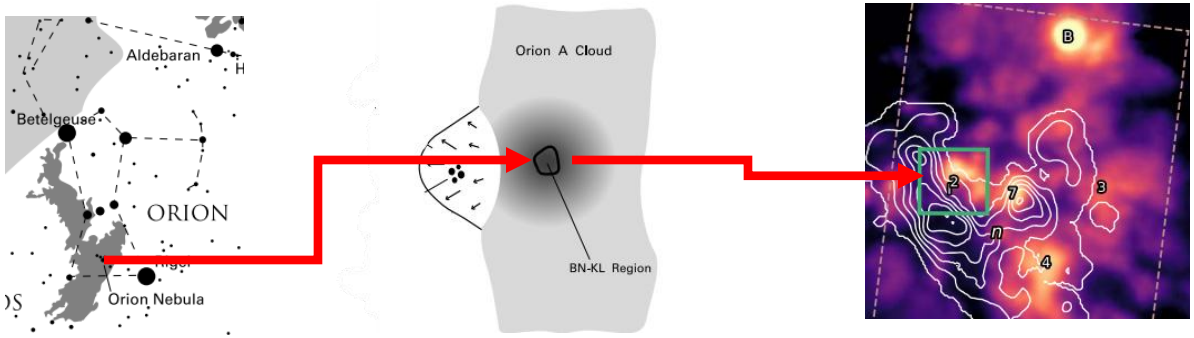

- **Two kinematic components**
  (About velocities relative to the LSR)
  - Blue Clump (blueshifted)
    −7.1 ± 0.7 km/s
  - Red Clump (redshifted)
    +1.4 ± 0.5 km/s

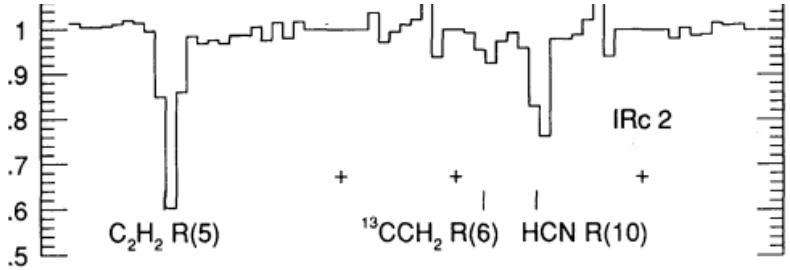

- **IRTF** : NASA Infrared Telescope Facility
  - 1990 – 1991 : 8 lines observed

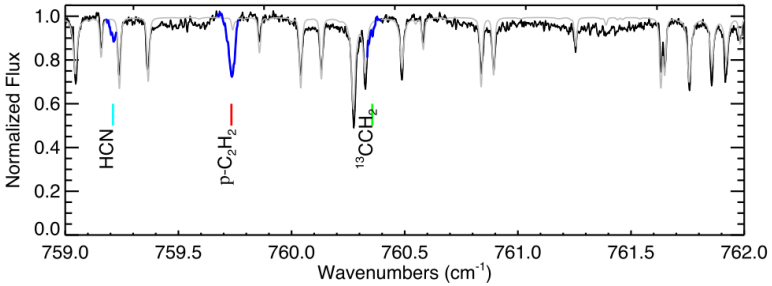

- **SOFIA** : Stratospheric Observatory for Infrared Astronomy
  - 2015 : 13 lines observed
  - 2018 – 2020 : 87 lines observed

- Stahler, S. W., & Palla, F. (2008). The formation of stars. John Wiley & Sons.
- Nickerson, Sarah, et al. "The mid-infrared molecular inventory toward orion IRc2." The Astrophysical Journal 945.1 (2023): 26.
- Evans, Neal J., J. H. Lacy, and John S. Carr. "Infrared molecular spectroscopy toward the Orion IRc2 and IRc7 sources-A new probe of physical conditions and abundances in molecular clouds.
- Rangwala, Naseem, et al. "High spectral resolution SOFIA/EXES observations of C2H2 toward orion IRc2." The Astrophysical Journal 856.1 (2018): 9.

Quantum chemical calculations : Infrared active and inactive

- Infrared absorption spectra
  - ✓ The motion corresponding to a normal mode must be accompanied by a change of electric dipole moment.
    - **Infrared active : Change of electric dipole moment.**
    - **Infrared inactive : No change of electric dipole moment.**
    - for example(Infrared active) : $^{12}C_2H_2(\nu_3, \nu_5)$, $^{13}CCH_2(\nu_1 \sim \nu_5)$
    - **Symmetric isotopologues of acetylene($^{12}C_2H_2$), two nuclear spin isomers (para(even) : ortho(odd) = 1:3) exist.**

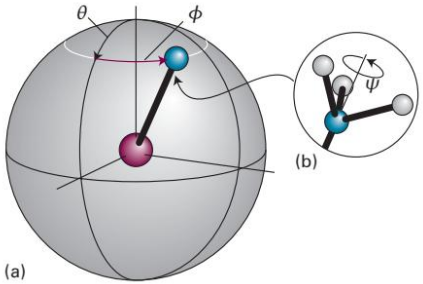

❖ **Normal modes of Acetylene : $3 \times 4 - 5 = 7 \Rightarrow 5$ (doubly degenerate)**

Label	Normal mode	Description	
ν_1	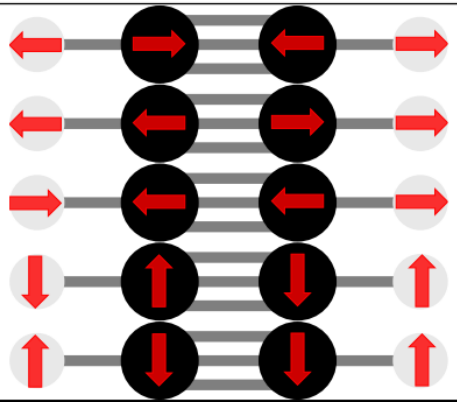	**CH** symmetric stretch	**(Infrared inactive)**
ν_2		**CC** symmetric stretch	**(Infrared inactive)**
ν_3		**CH** antisymmetric stretch	**(Infrared active)**
ν_4		Symmetric bend	**(Infrared inactive, doubly degenerate)**
ν_5		Antisymmetric bend	**(Infrared active, doubly degenerate)**

Normal modes of Acetylene

- McQuarrie, D. A. (2008). Quantum chemistry. University Science Books.
- Atkins, P. W., De Paula, J., & Keeler, J. (2023). Atkins' physical chemistry. Oxford university press.
- Herman, Michel. "The acetylene ground state saga." Molecular Physics 105.17-18 (2007): 2217-2241.

Why Study the Mid-Infrared Region?

- C_2H_2 has **no permanent dipole moment**, it cannot be observed via rotational transitions at radio wavelengths like CO or HCN.
- C_2H_2 can only be studied in the mid-infrared (MIR; 5~28 μm), where its ro-vibrational transitions.
- Its v_5 ro-vibration band at 13.7 μm is the strongest

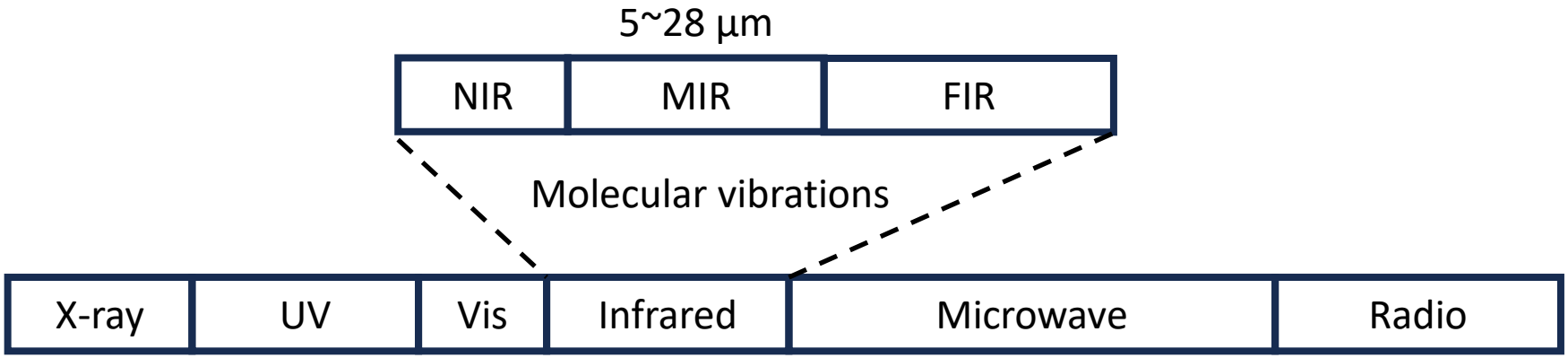

- **Chemical Conventions**
  - Wavenumber

$$\tilde{v}(cm^{-1}) = \frac{v}{c}$$

  - Rotational energy

$$E_J = \frac{J(J+1)\hbar^2}{2I} = hc\tilde{B}J(J+1)$$

    - J: angular momentum quantum number
  - Moment of inertia

$$I = \sum_i m_i x_i^2$$

  - rotational constant

$$\tilde{B}(cm^{-1}) = \frac{\hbar}{4\pi cI}$$

    - ✓ $\text{wavenumber}[\text{cm}^{-1}] = \frac{10^4}{\lambda[\mu\text{m}]}$

- Rangwala, Naseem, et al. "High spectral resolution SOFIA/EXES observations of C2H2 toward orion IRc2." The Astrophysical Journal 856.1 (2018): 9.

Symbol	Description
$\tilde{S}$	Ro-Vibration terms
$\tilde{G}$	Vibrational terms
$\tilde{F}$	Rotational terms
$\tilde{\nu}_P, \tilde{\nu}_R, \tilde{\nu}_Q$	Spectral branches(P, R, Q)

$$\tilde{S} = \tilde{G} + \tilde{F} \quad , \quad \begin{cases} \tilde{G} = \left(\nu + \frac{1}{2}\right)\tilde{\nu} \\ \tilde{F} = \tilde{B}J(J+1) \end{cases}$$

❖ ν_i (vibrational quantum number)= 0,1,2, …

$$\tilde{\nu}_P = \tilde{S}(\nu_0 + 1, \tilde{\nu}, \tilde{B}, J-1) - \tilde{S}(\nu_0, \tilde{\nu}, \tilde{B}, J) = \tilde{\nu} - 2\tilde{B}J$$

$$\tilde{\nu}_Q = \tilde{S}(\nu_0 + 1, \tilde{\nu}, \tilde{B}, J) - \tilde{S}(\nu_0, \tilde{\nu}, \tilde{B}, J) = \tilde{\nu}$$

$$\tilde{\nu}_R = \tilde{S}(\nu_0 + 1, \tilde{\nu}, \tilde{B}, J+1) - \tilde{S}(\nu_0, \tilde{\nu}, \tilde{B}, J) = \tilde{\nu} + 2\tilde{B}(J+1)$$

J state

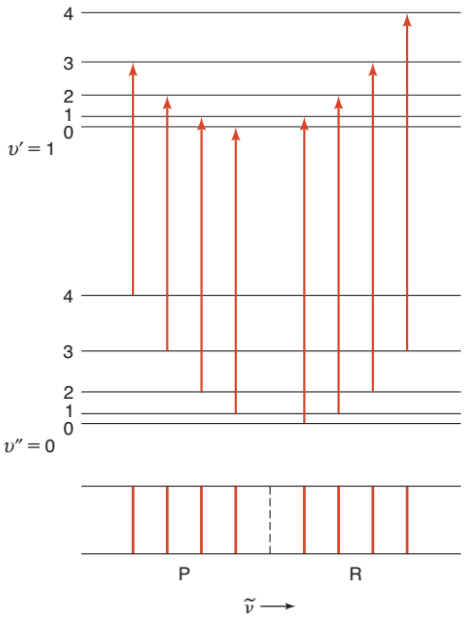

❖ **Partition function**

$$Q_{rot} = \sum_{J_S=0}^{\infty} (2J_S + 1) \exp\left(-\frac{E_J}{kT}\right)$$

- Atkins, P. W., De Paula, J., & Keeler, J. (2023). Atkins' physical chemistry. Oxford university press.
- Chang, R., & Thoman Jr, J. W. (2014). Physical chemistry for the chemical sciences. Royal Society of Chemistry.

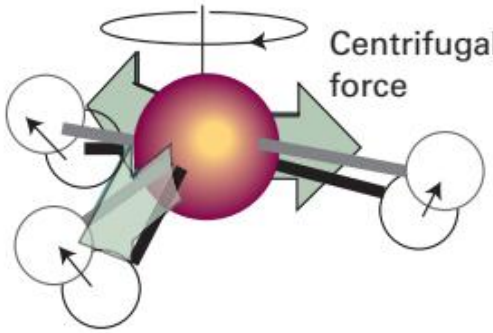

$$\tilde{F} = \tilde{B}J(J+1) \quad -\tilde{D}_J J^2(J+1)^2$$

$$\tilde{B} = \frac{\hbar}{4\pi c I}$$

A molecule is not a rigid body!

Molecular rotation

- Increase in bond length of molecules
- Increase in moment of inertia
- Decrease in rotational constant
- Decrease in rotational energy

Centrifugal distortion constant

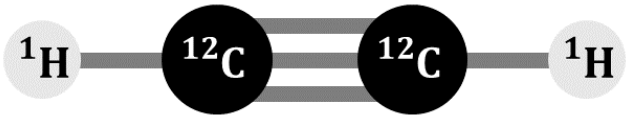

$$\tilde{D}_J = \frac{4\tilde{B}^3}{\tilde{\nu}^2}$$ **(linear rotor)**

- Atkins, P. W., De Paula, J., & Keeler, J. (2023). Atkins' physical chemistry. Oxford university press.

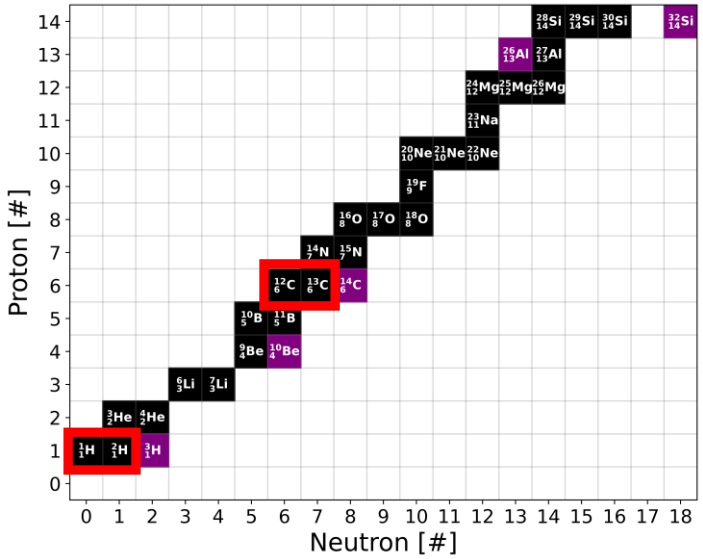

- **Isotopes : NNDC (half-life)**

$^{3}_{1}\mathrm{H}$: 12.32 y

$^{10}_{4}\mathrm{Be}$: 1.51×10^{6} y

$^{14}_{6}\mathrm{C}$: 5700 y

$^{26}_{13}\mathrm{Al}$: 7.17×10^{5} y

$^{32}_{14}\mathrm{Si}$: 153 y

- All quantum chemical calculations were performed using the **Gaussian16**

Num. [#]	Structure	Method FSF = 1.0000	ν_1 [cm^{-1}]	ν_2 [cm^{-1}]	ν_3 [cm^{-1}]	ν_4 [cm^{-1}]	ν_5 [cm^{-1}]	$\bar{B}$ [cm^{-1}]
0		HF	3719.692	2246.893	3607.484	793.610	882.237	1.2113
		B3LYP	3542.390	2087.886	3442.297	534.175	774.627	1.1766
		PBE0	3563.447	2102.532	3460.432	575.732	780.424	1.1770
		MP2	3568.687	2001.497	3480.443	374.534	747.863	1.1585
1		HF	3705.880	2211.601	3601.439	787.455	880.998	1.1824
		B3LYP	3529.920	2054.704	3436.511	530.081	773.484	1.1485
		PBE0	3550.771	2069.187	3454.626	571.308	779.278	1.1489
		MP2	3557.340	1969.037	3474.553	371.702	746.750	1.1307
2		HF	3670.580	2082.710	2843.301	657.380	837.488	1.0184
		B3LYP	3498.078	1946.382	2695.795	466.499	697.315	0.9901
		PBE0	3517.957	1958.769	2712.453	499.230	707.655	0.9903
		MP2	3528.849	1883.762	2696.072	332.028	662.589	0.9762
3		HF	3691.056	2175.212	3596.685	781.435	879.596	1.1529
		B3LYP	3516.414	2020.534	3431.992	526.002	772.308	1.1197
		PBE0	3537.079	2034.844	3450.073	566.906	778.088	1.1201
		MP2	3544.806	1935.681	3470.024	368.870	745.624	1.1022
4		HF	3650.710	2053.231	2836.946	655.611	831.742	0.9935
		B3LYP	3479.841	1917.850	2690.606	463.780	694.732	0.9659
		PBE0	3499.486	1930.164	2707.181	496.565	704.675	0.9661
		MP2	3511.667	1854.562	2692.251	329.755	660.872	0.9522
5		HF	3668.247	2067.710	2803.612	648.627	837.200	1.0018
		B3LYP	3496.169	1930.915	2659.920	460.335	697.020	0.9740
		PBE0	3515.974	1943.344	2676.210	492.517	707.511	0.9742
		MP2	3527.424	1866.274	2663.404	327.934	661.778	0.9601
6	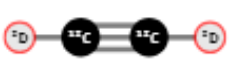	HF	2997.782	1972.156	2648.723	647.765	662.808	0.8692
		B3LYP	2833.916	1846.155	2527.438	445.952	568.754	0.8457
		PBE0	2853.342	1857.424	2540.753	480.778	573.011	0.8458
		MP2	2817.727	1793.148	2555.446	312.166	549.103	0.8346
7		HF	3648.706	2036.737	2797.652	646.773	831.499	0.9764
		B3LYP	3478.197	1901.036	2655.100	457.617	694.411	0.9491
		PBE0	3497.776	1913.382	2671.303	489.848	704.507	0.9493
		MP2	3510.435	1835.879	2659.907	325.662	660.044	0.9355
8		HF	2965.050	1955.340	2640.730	644.736	656.746	0.8542
		B3LYP	2804.642	1829.336	2519.795	441.000	567.229	0.8310
		PBE0	2823.697	1840.609	2533.075	475.411	571.500	0.8311
		MP2	2791.728	1774.858	2547.684	308.749	547.595	0.8201
9		HF	2931.432	1937.423	2633.996	644.163	648.181	0.8387
		B3LYP	2774.495	1811.482	2513.385	436.132	565.592	0.8160
		PBE0	2793.182	1822.756	2526.626	470.176	569.825	0.8160
		MP2	2764.762	1755.579	2541.237	305.350	546.050	0.8050

- **TOPSEGI** : **Python**-based software package developed to improve the accuracy of molecular **temperature and column density** estimations in **interstellar environments**
  - **Lee, M., Park, J., Oh, S., Cheoun, M.K., Park, S.Y., 2025(arXiv:2501.15824).**
  - **The package is implemented in Python 3 and is freely available on GitHub at https://github.com/BrownNo28/ISM.**
- **Chojeong, in central Korea, is my hometown !**

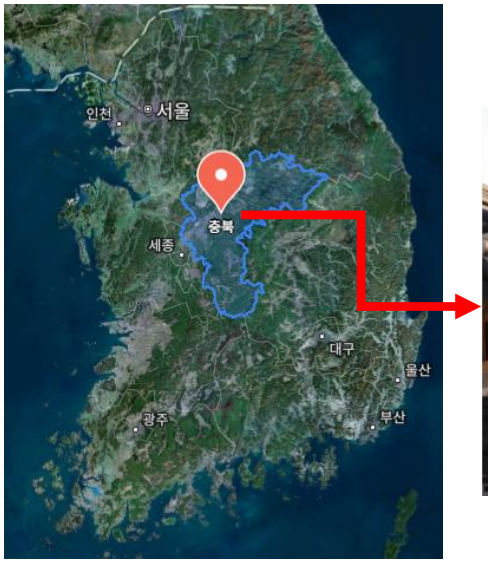

椒井行宮

椒井藥水

- Originates from a **dialect in central Korea**, meaning "**dust(ほこり)**" or "**tiny particles**".
- This name symbolizes the focus on **analyzing molecular components**, which, like dust in the universe, are the fundamental building blocks of the **ISM**.

M42
(Orion Nebula)

- map.naver.com/, ko.wikipedia.org/, www.kctg.or.kr/

➢ Rotation Diagram (Traditional)

Single-parameter fitting

- Assuming LTE(Local Thermodynamic Equilibrium)

$$\ln\frac{N_j}{g_j} = -\frac{1}{T_{ex}}\frac{E_l}{k} + \ln\frac{N}{Q_R(T_{ex})}$$

$$y = ax + b$$

✦ Analysis Tool : Rotation Diagram
✦ Structure : (0). C_2H_2, symmetric(odd)

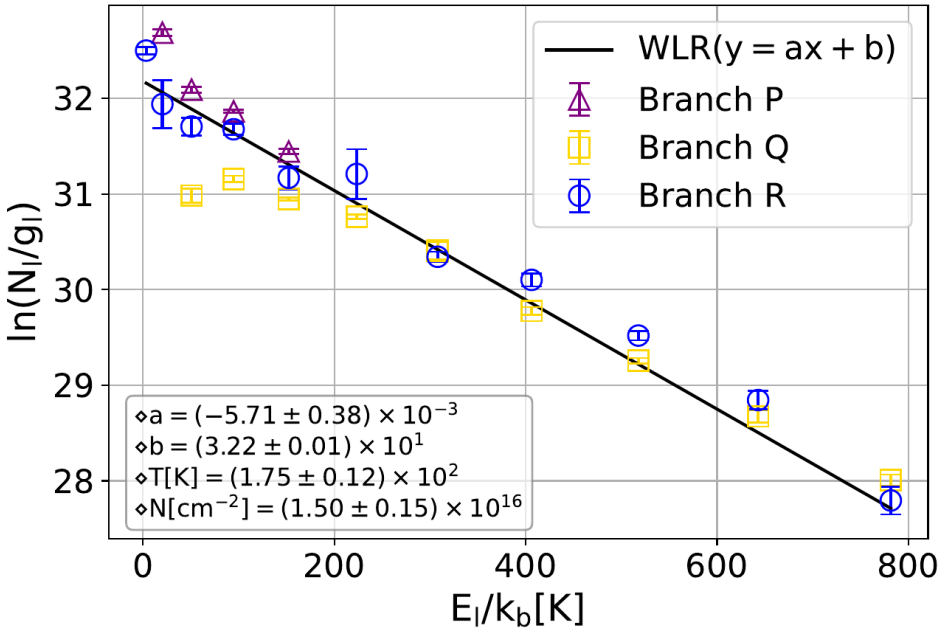

➢ Quadtree : 2D-optimization algorithm(This work)

Two-parameter fitting

$$\chi^2 = \sum_{\text{obs } l}\left(\frac{N_l^{\text{theo}} - N_l^{\text{obs}}}{\sigma_l^{\text{obs}}}\right)^2 ; N_l^{\text{theo}} = N\frac{g_l}{Q(T)}\exp\left(-\frac{E_l}{k_B T}\right)$$

$$\mathrm{N}_i^{\text{theo}} = \mathrm{N}_i^{\text{theo}}(\mathrm{N},\mathrm{T}) \qquad \text{Quadtree Node}_{\max}(h) = \sum_{k=0}^{h} 4^k$$

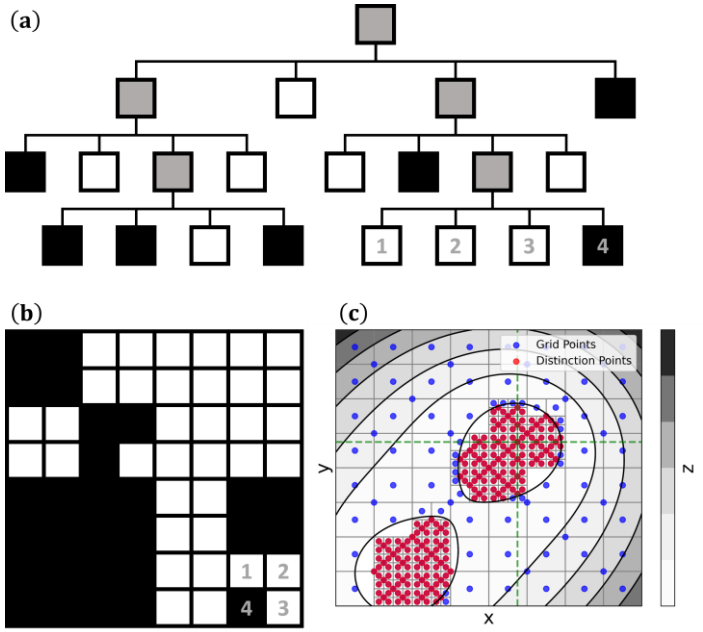

- Goldsmith, P. F., & Langer, W. D. 1999, The AstrophysicalJournal, 517, 209
- Nickerson, Sarah, et al. "The mid-infrared molecular inventory toward orion IRc2." The Astrophysical Journal 945.1 (2023): 26.

➢ Select C_2H_2 and Its Isotopologues

HITRAN

TOPSEGI

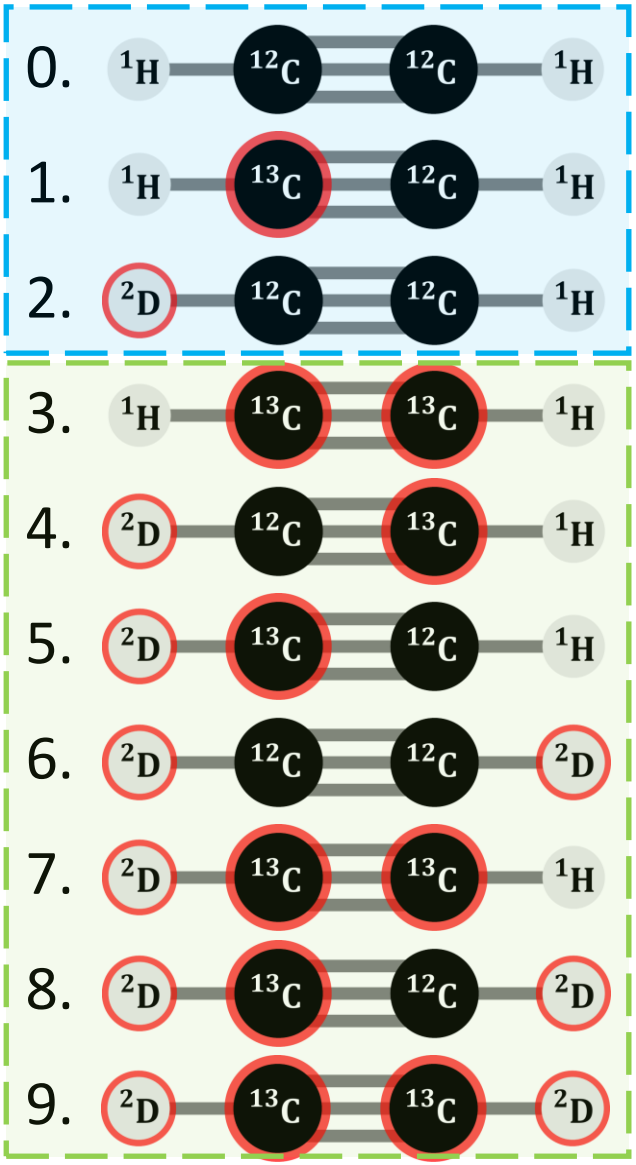

❖ HITRAN

(***hi*gh-**

resolution *tran*smission

molecular absorption

database)

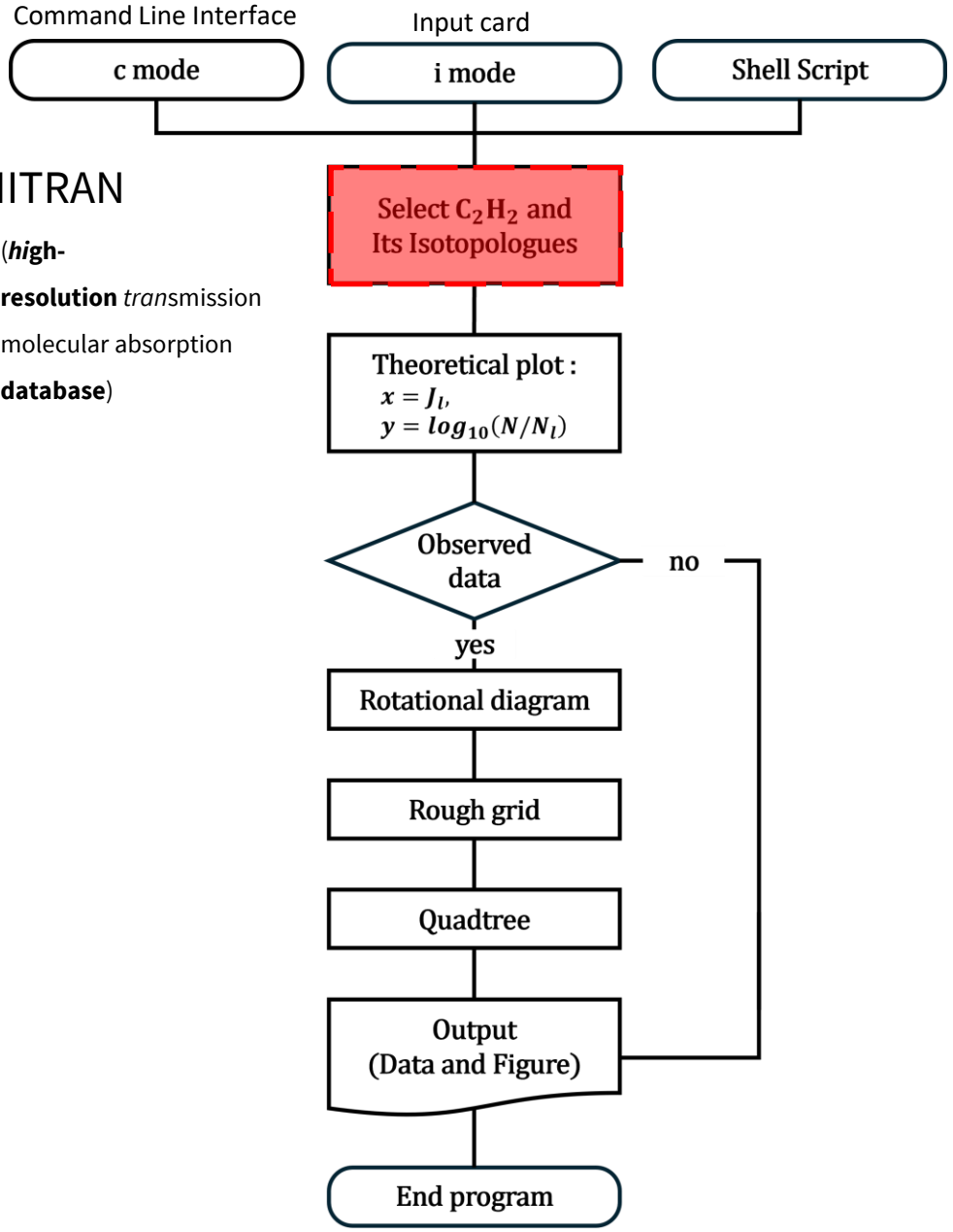

➢ Theoretical plot

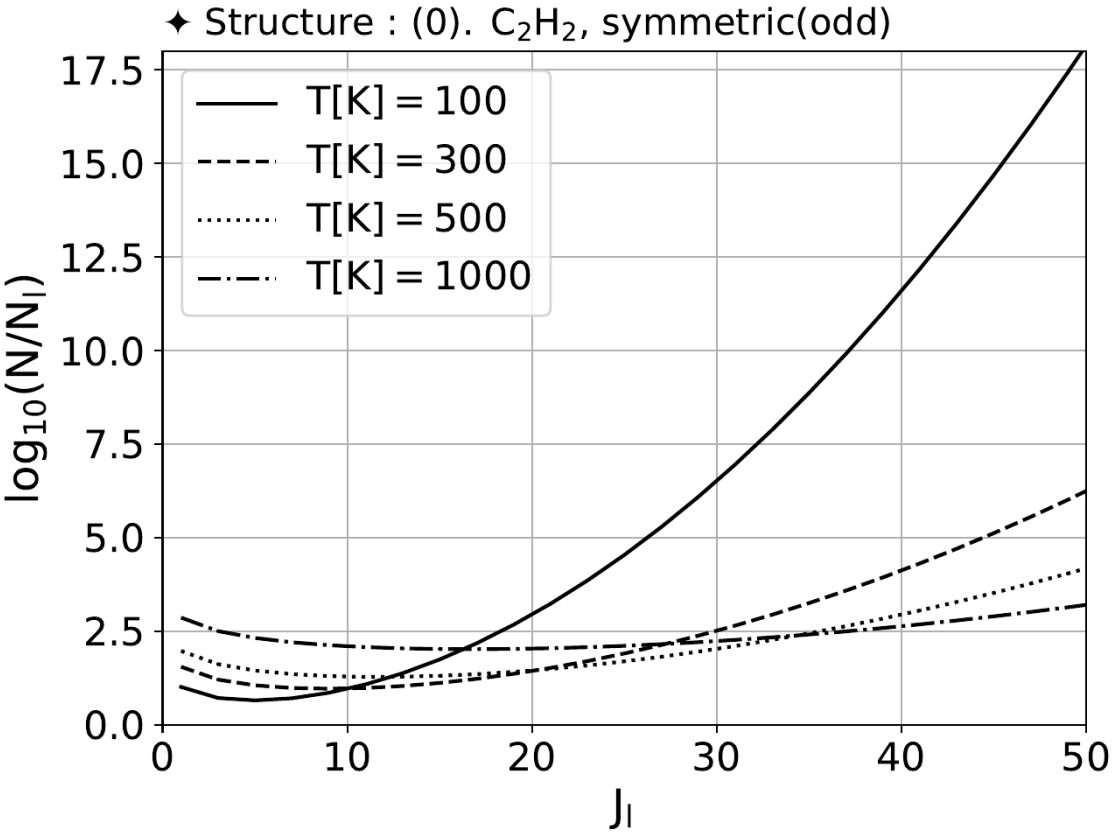

Predict spectra without observations

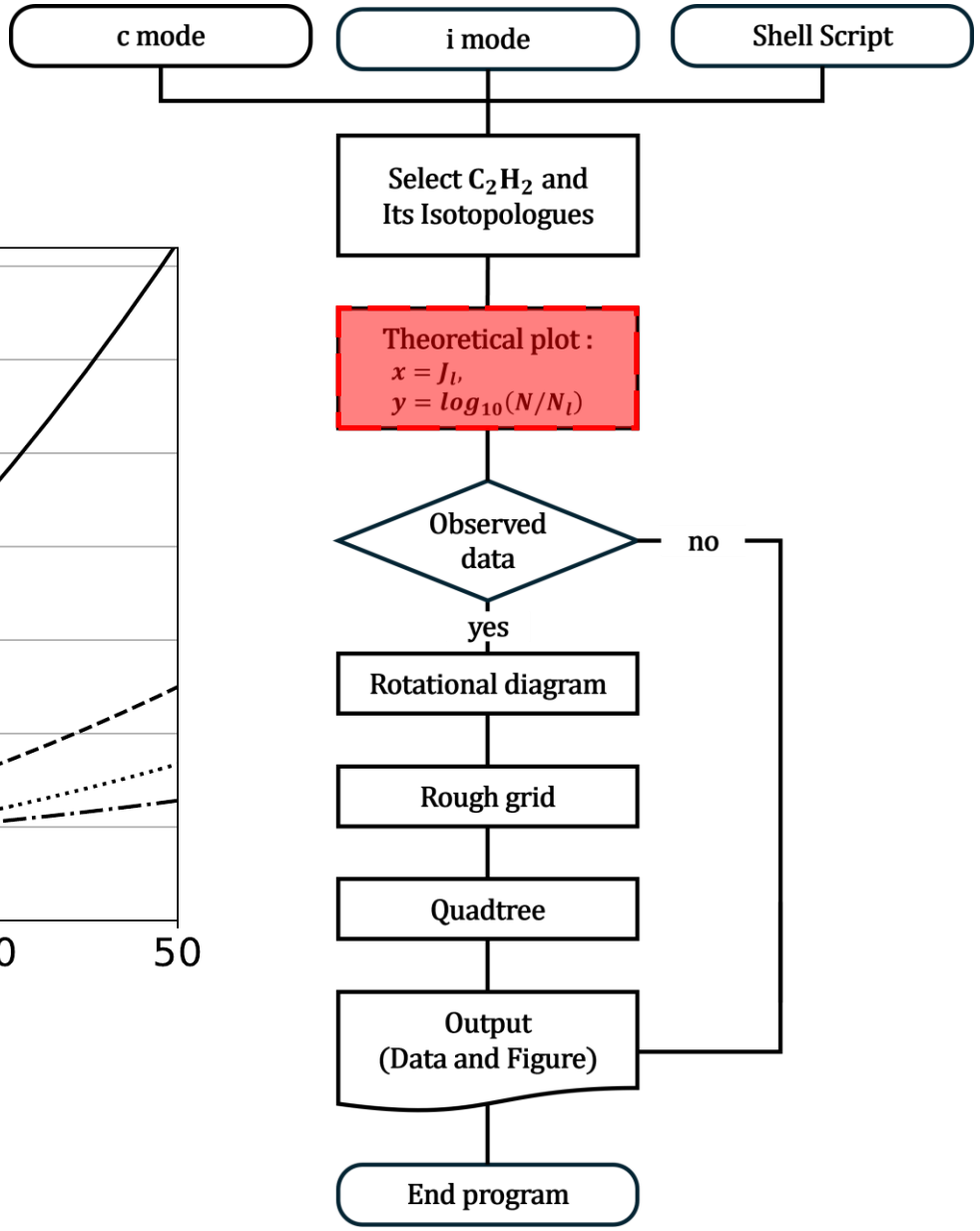

➢ Rotational diagram

- Assuming LTE(Local Thermodynamic Equilibrium)

$$\ln\left(\frac{N_l}{g_l}\right) = -\frac{1}{T}\left(\frac{E_l}{k_B}\right) + \ln\left(\frac{N}{Q(T)}\right), \quad y = ax + b$$

$$T = -\frac{1}{a}, \qquad T_{err} = \frac{a_{err}}{a^2}$$

$$N = Q(T)e^b, \quad N_{err} = Nb_{err}$$

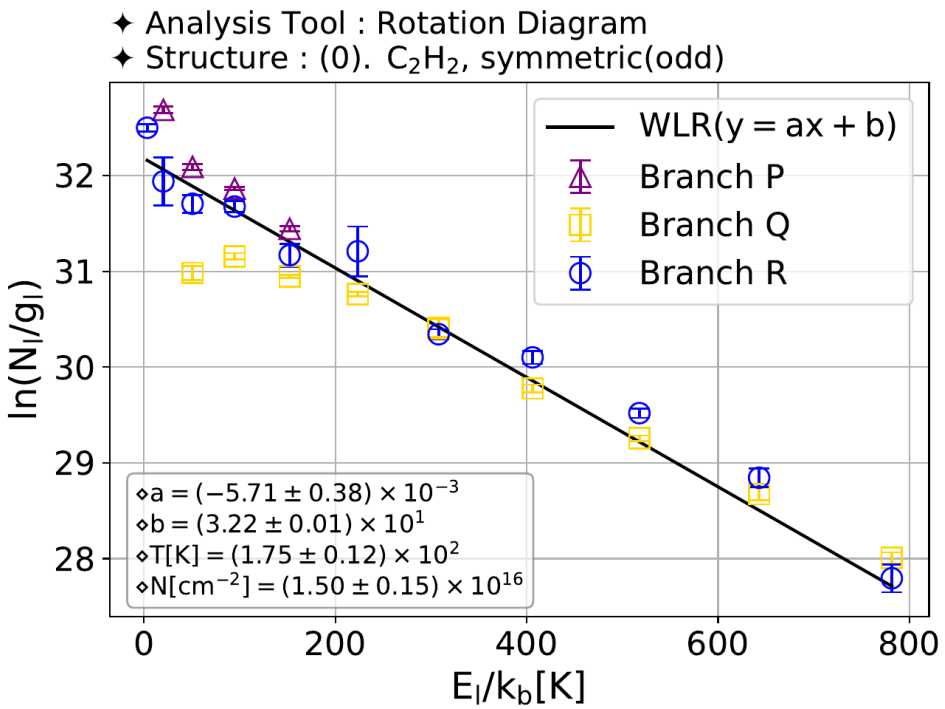

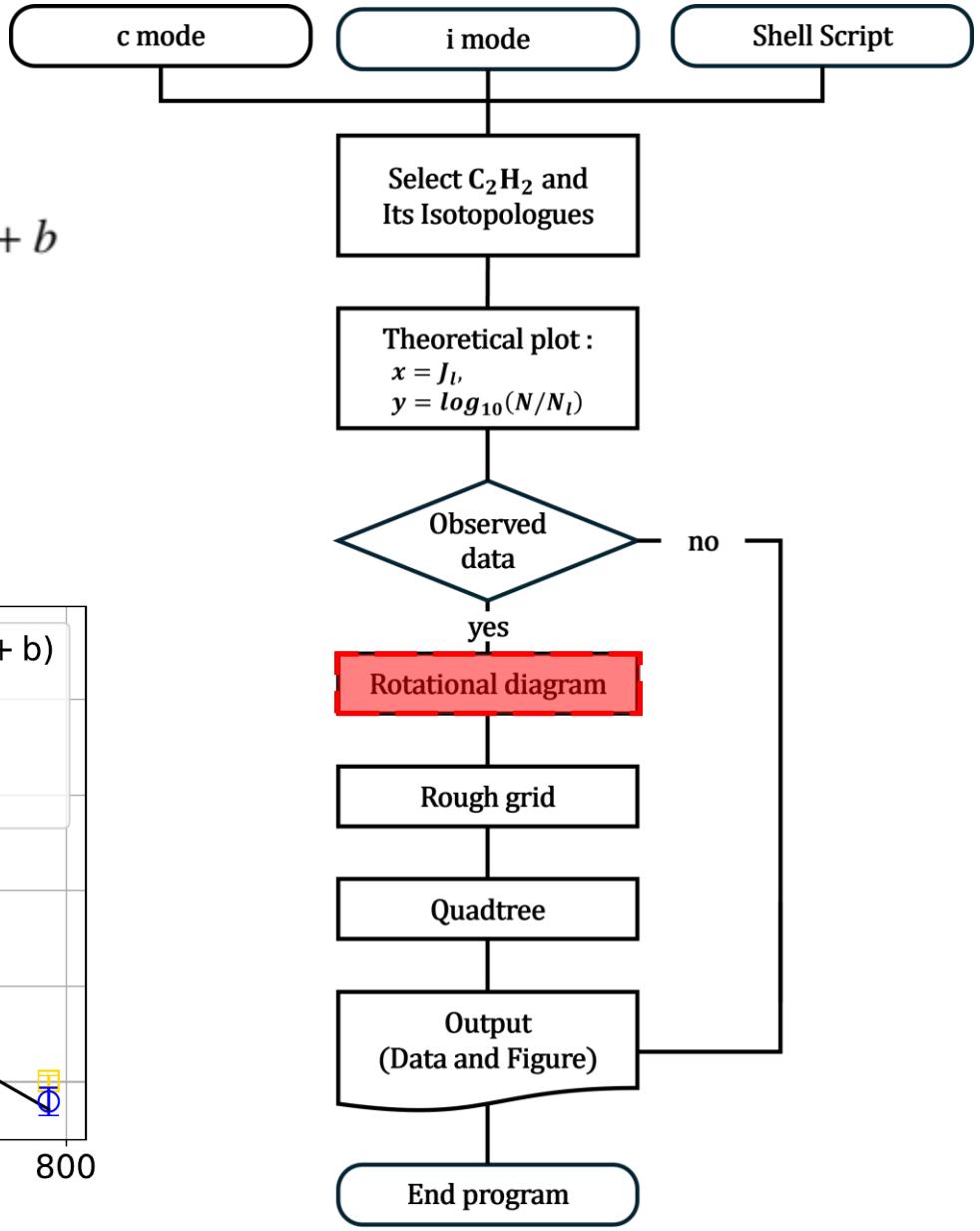

➢ Rough grid

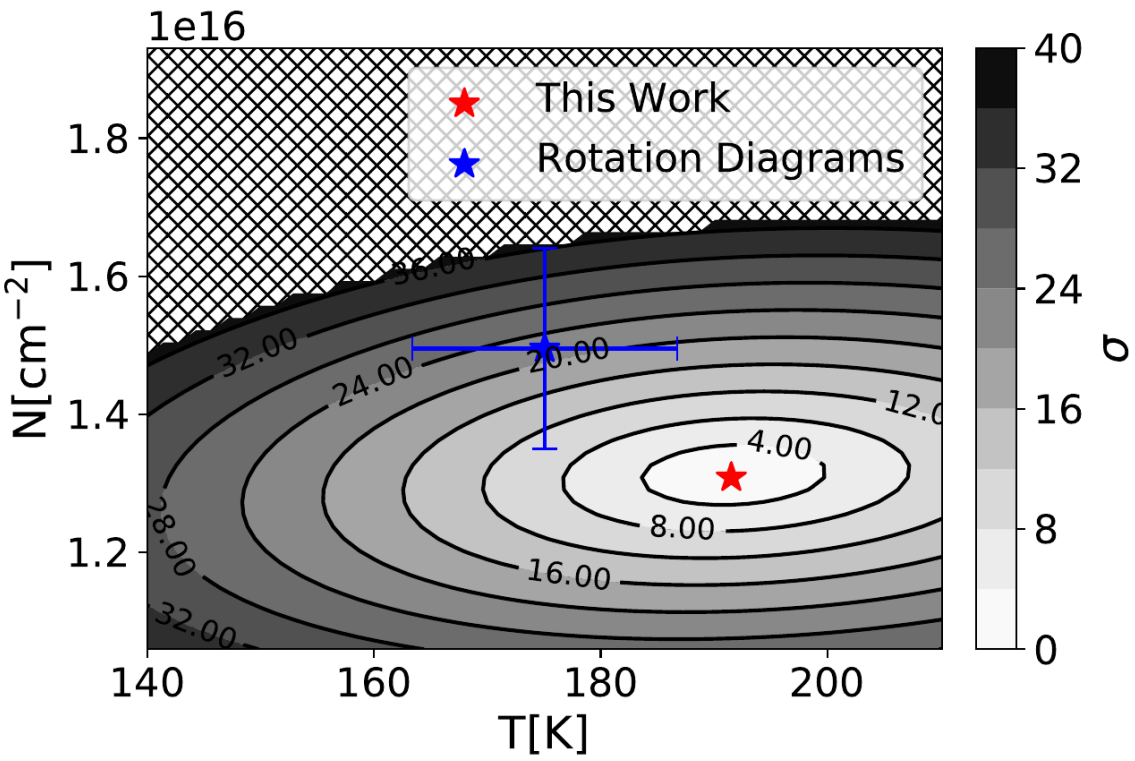

The **X-shaped hatching** indicates regions where Δχ2 is too large, making numerical calculations infeasible.

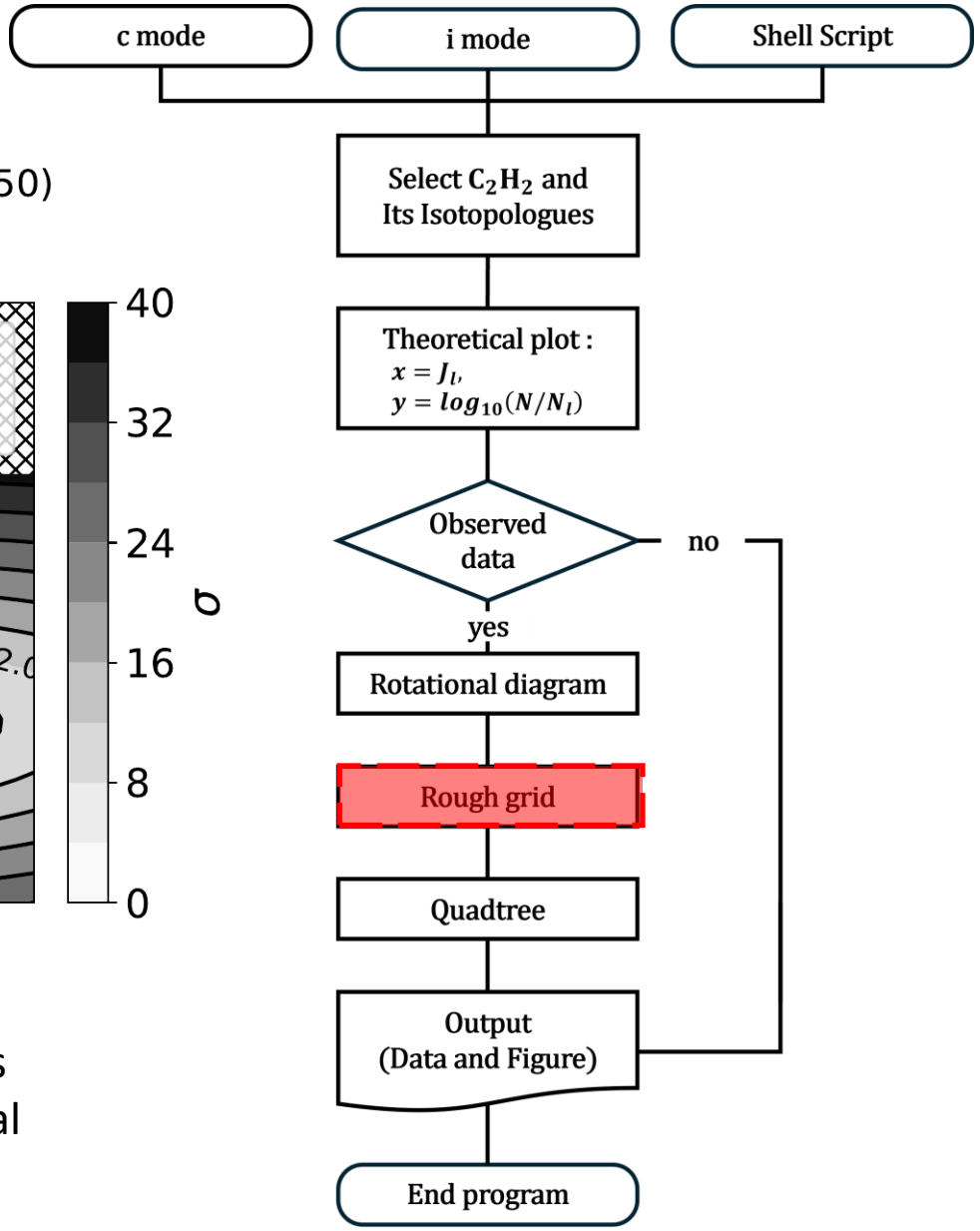

➢ Quadtree

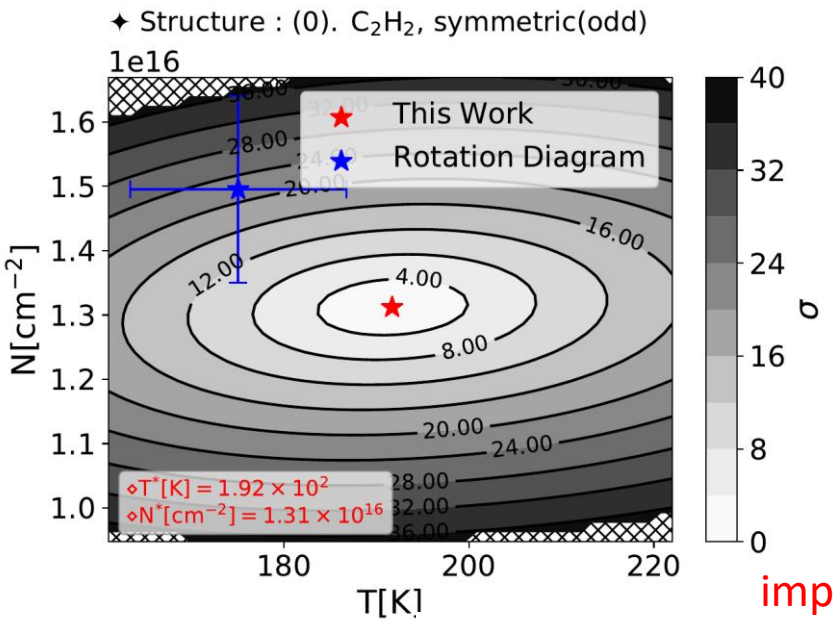

improved precision

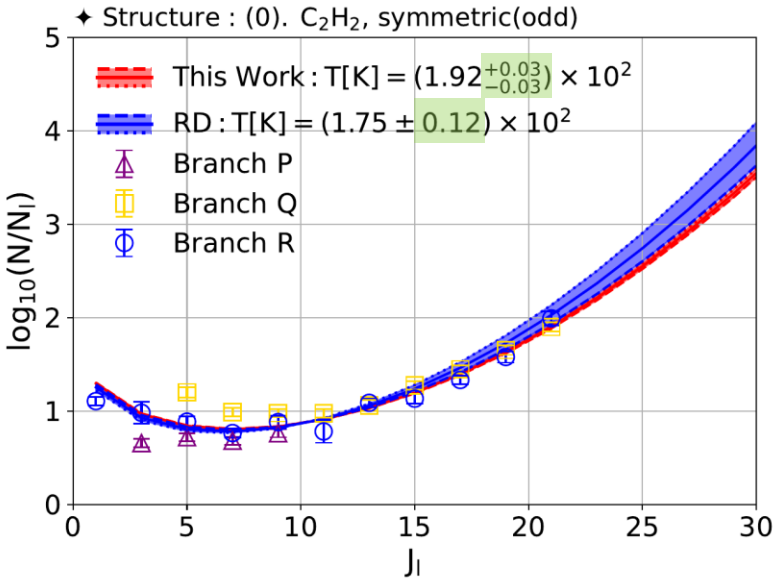

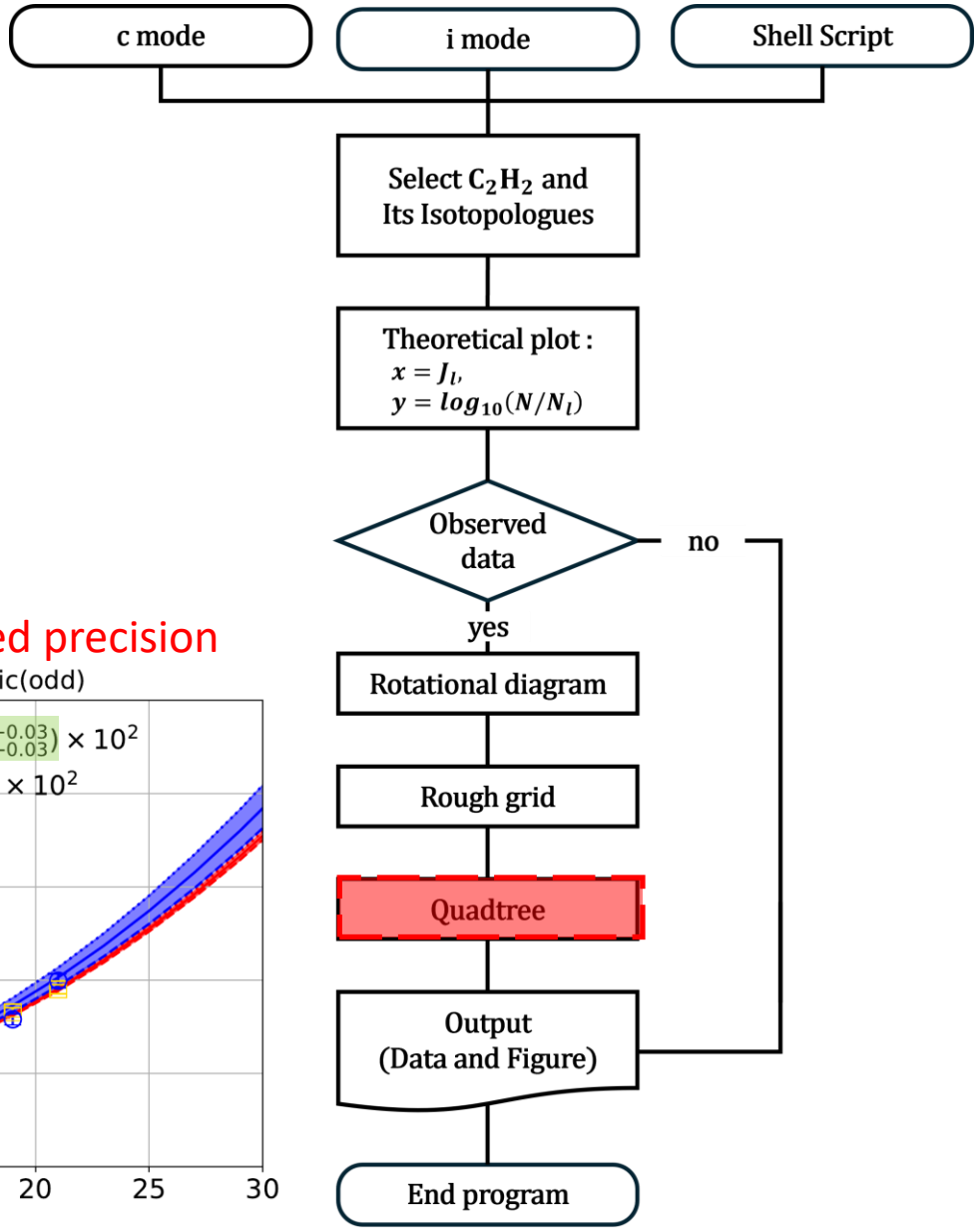

Species	Source	Estimated Temperature T (K)	Estimated Column Density N (cm^{-2})	Method
		Blue Clump		
C_2H_2 (even, Para)	Nickerson et al. (2023)	145 ± 9	$(1.23 \pm 0.15) \times 10^{16}$	RD
	This work	161^{+3}_{-3}	$(0.983^{+0.019}_{-0.018}) \times 10^{16}$	χ^2
C_2H_2 (odd, Ortho)	Nickerson et al. (2023)	175 ± 12	$(1.50 \pm 0.15) \times 10^{16}$	RD
	This work	192^{+3}_{-3}	$(1.31^{+0.015}_{-0.014}) \times 10^{16}$	χ^2
$^{13}CCH_2$	Nickerson et al. (2023)	91 ± 9	$(2.56 \pm 0.18) \times 10^{15}$	RD
	This work	$87.1^{+12.3}_{-10.4}$	$(2.45^{+0.20}_{-0.19}) \times 10^{15}$	χ^2
		Red Clump		
C_2H_2 (even, Para)	Nickerson et al. (2023)	158 ± 16	$(3.09 \pm 0.57) \times 10^{15}$	RD
	This work	170^{+11}_{-10}	$(2.43^{+0.18}_{-0.18}) \times 10^{15}$	χ^2
C_2H_2 (odd, Ortho)	Nickerson et al. (2023)	229 ± 27	$(3.58 \pm 0.71) \times 10^{15}$	RD
	This work	270^{+21}_{-19}	$(2.65^{+0.17}_{-0.16}) \times 10^{15}$	χ^2
$^{13}CCH_2$	Nickerson et al. (2023)	64 ± 6	$(6.74 \pm 0.64) \times 10^{14}$	RD
	This work	$64.4^{+70.7}_{-23.4}$	$(6.69^{+1.98}_{-1.66}) \times 10^{14}$	χ^2

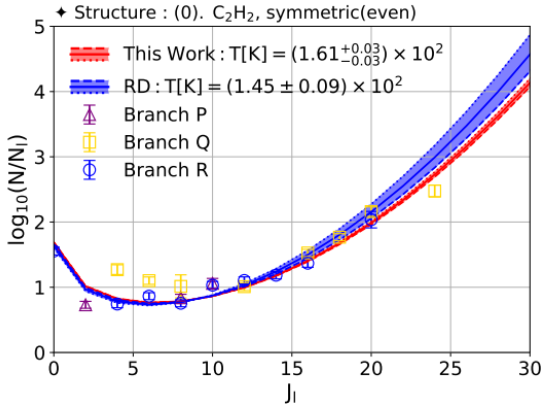

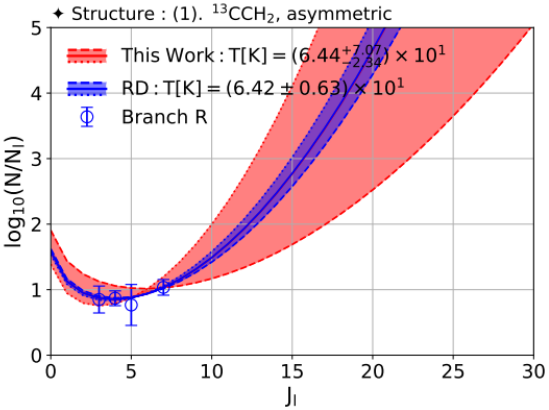

- The increase in uncertainty arises from the limited number of observational data points (four) used in the fitting process.

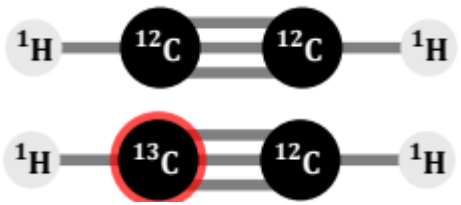

$$\frac{^{12}C}{^{13}C} = \frac{2\,(N(\mathrm{Ortho}-C_2H_2) + N(\mathrm{Para}-C_2H_2))}{N(^{13}CCH_2)}$$

Source \ Clump	Blue Clump	Method	Red Clump	Method
Nickerson et al. (2023) ($^{12}C/^{13}C$)	21.3 ± 2.2	RD	19.8 ± 3.4	RD
This Work ($^{12}C/^{13}C$)	$18.72^{+1.54}_{-1.46}$	χ^2	$15.07^{+1.61}_{-1.60}$	χ^2 (^{12}C) + RD (^{13}C)

The RD method overestimates the 12C/13C ratio.

Result (example : pseudo data of 13C2H2)

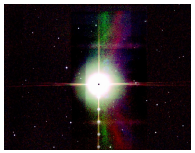

For instance, astronomical environments such as Y CVn : 3.5 (12C/13C) ≈ 22.2%($\frac{13C}{12C+13C}$)

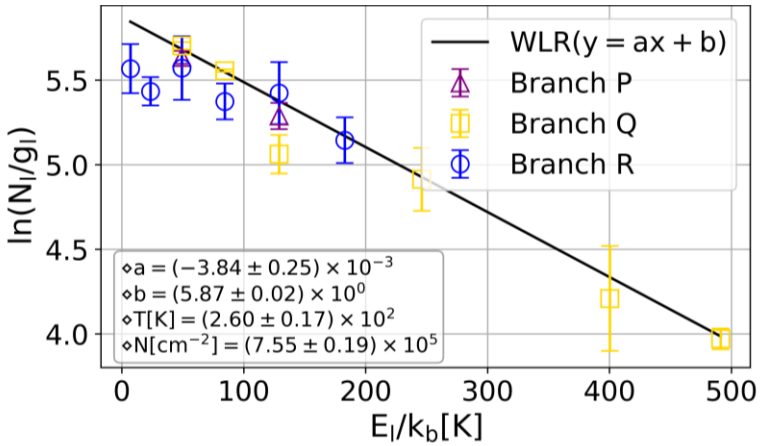

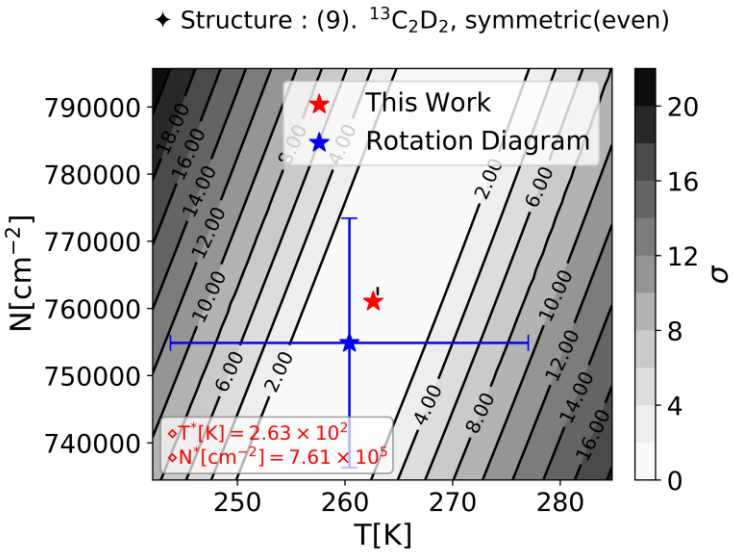

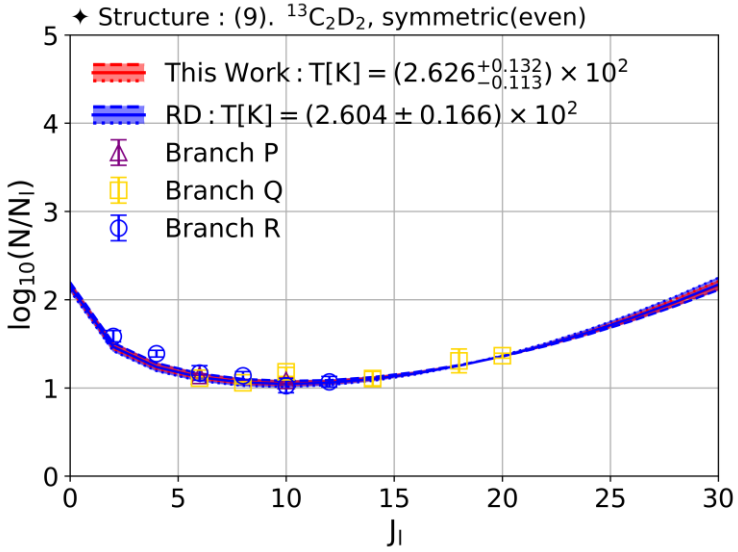

Future work : HNC

Table 2. Observed ν_2 band HNC Transitions and Inferred Parameters

Transition	Wavenumber (cm^{-1})	E_l/k_b (K)	g_l	v_{LSR} (km s^{-1})	τ_0	N_l $\times 10^{14} cm^{-2}$
P3e	453.64798	26.1	42	−6.8±0.3	0.031±0.003	1.09±0.20
P5e	447.5964	65.3	66	−7.0±0.2	0.041±0.001	0.94±0.05
P6e	444.57022	91.4	78	−5.3±0.4	0.029±0.003	0.86±0.19
P7e	441.54388	121.8	90	−9.1±0.3	0.031±0.003	0.65±0.11
P8e	438.51747	156.6	102	−7.9±0.3	0.028±0.002	0.64±0.08
Q1e	462.74319	4.4	18	−8.9±0.2	0.057±0.003	0.46±0.04
Q2e	462.78519	13.1	30	−8.1±0.2	0.071±0.004	0.71±0.10
Q3e	462.84818	26.1	42	−8.9±0.1	0.080±0.003	0.73±0.06
Q4e	462.93214	43.5	54	−8.4±0.2	0.080±0.003	0.72±0.05
Q5e	463.03705	65.3	66	−8.3±0.1	0.082±0.002	0.69±0.04
Q6e	463.16287	91.4	78	−8.4±0.2	0.078±0.003	0.81±0.04
Q8e	463.47714	156.6	102	−7.7±0.2	0.055±0.003	0.54±0.06
Q9e	463.66551	195.8	114	−7.7±0.3	0.037±0.002	0.30±0.04
Q11e	464.10446	287.1	138	−8.1±0.5	0.022±0.005	0.13±0.07
Q12e	464.35494	339.3	150	−5.9±0.6	0.013±0.002	0.09±0.02
R0e	465.74576	0.0	6	−8.3±0.3	0.037±0.003	0.17±0.03
R1e	468.76863	4.4	18	−8.0±0.2	0.069±0.003	0.79±0.05
R2e	471.7907	13.1	30	−8.1±0.2	0.076±0.003	0.92±0.08
R3e	474.8119	26.1	42	−8.0±0.2	0.081±0.003	1.01±0.08
R5e	480.85136	65.3	66	−8.2±0.2	0.071±0.003	0.81±0.04
R7e	486.88636	121.8	90	−7.7±0.3	0.048±0.003	0.78±0.07
R8e	489.902	156.6	102	−6.2±0.3	0.042±0.003	0.51±0.08
R9e	492.91629	195.8	114	−7.8±0.3	0.043±0.002	0.75±0.06
R10e	495.92916	239.3	126	−5.9±0.5	0.026±0.004	0.30±0.07

Table 3. Observed ν_2 band $H^{13}CN$ Transitions and Inferred Parameters

Transition	Wavenumber (cm^{-1})	E_l/k_b (K)	g_l	v_{LSR} (km s^{-1})	τ_0	N_l $\times 10^{14} cm^{-2}$
R1e	711.72312	4.1	36	−7.5±0.4	0.059±0.005	2.46±0.27
R6e	726.098321	87.0	156	−6.5±0.2	0.083±0.005	5.30±0.44
R8e	731.839651	149.2	204	−5.7±0.3	0.054±0.005	3.05±0.40

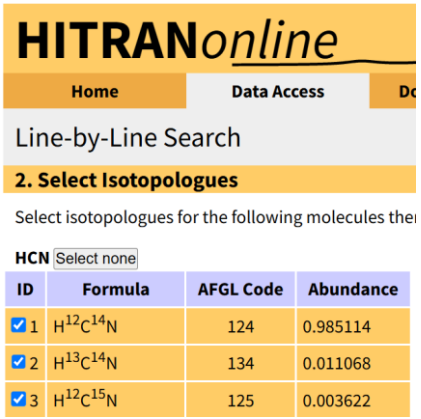

ID	Formula
1	$^{1}H^{12}C^{14}N$
2	$^{1}H^{13}C^{14}N$
3	$^{1}H^{12}C^{15}N$
4	$^{2}D^{12}C^{14}N$
5	$^{2}D^{13}C^{14}N$
6	$^{1}H^{13}C^{15}N$
7	$^{2}D^{12}C^{15}N$
8	$^{2}D^{13}C^{15}N$

- https://hitran.org/
- Nickerson, Sarah, et al. "The first mid-infrared detection of HNC in the interstellar medium: Probing the extreme environment toward the orion hot core." The Astrophysical Journal 907.1 (2021): 51.

Summary

- Acetylene is among the simplest organic molecules found abundantly in outer space.

- 12C/13C is an important diagnostic tool for probing the Galactic chemical evolution or simply the nucleosynthesis history of the Galaxy. (AGB Star => (12C(p,γ)13N(β+)13C))

- The rotational diagram (RD) method overestimates the 13C/12C ratio, while the χ^2 method reduces uncertainties for more accurate and reliable results.

Source \ Clump	Blue Clump	Method	Red Clump	Method
Nickerson et al. (2023) ($^{12}C/^{13}C$)	21.3 ± 2.2	RD	19.8 ± 3.4	RD
This Work ($^{12}C/^{13}C$)	$18.72^{+1.54}_{-1.46}$	χ^2	$15.07^{+1.61}_{-1.60}$	χ^2 (^{12}C) + RD (^{13}C)

- The RD method **overestimates** the 12C/13C ratio.
- TOPSEGI (Python package) developed in this study facilitates efficient χ2 fitting and isotopic ratio analysis.

- Future work will expand to include the analysis of molecules and isotopologues in space, such as HCN.


Thank you for your attention